The (oxo)[(2,3,7,8,12,13,17,18-octachloro-5,10,15,20-tetrakis(4-tolylporphyrinato)]vanadium(IV): Synthesis, UV–visible, Cyclic voltammetry and X-ray crystal structure

C. Mchiri, N. Amiri, S. Jabli, T. Roisnel, H. Nasri

The preparation of the oxo vanadium(IV) complex of 2,3,7,8,12,13,17,18-octachloro-5,10,15,20-tetrakis(4-tolylporphyrin) with the formula [V(Cl$_8$TTP)O] is described. The presence of chlorine atoms at the β-pyrrole positions of the porphyrin have a very important role on the electronic and structural properties of [V(Cl$_8$TTP)O].
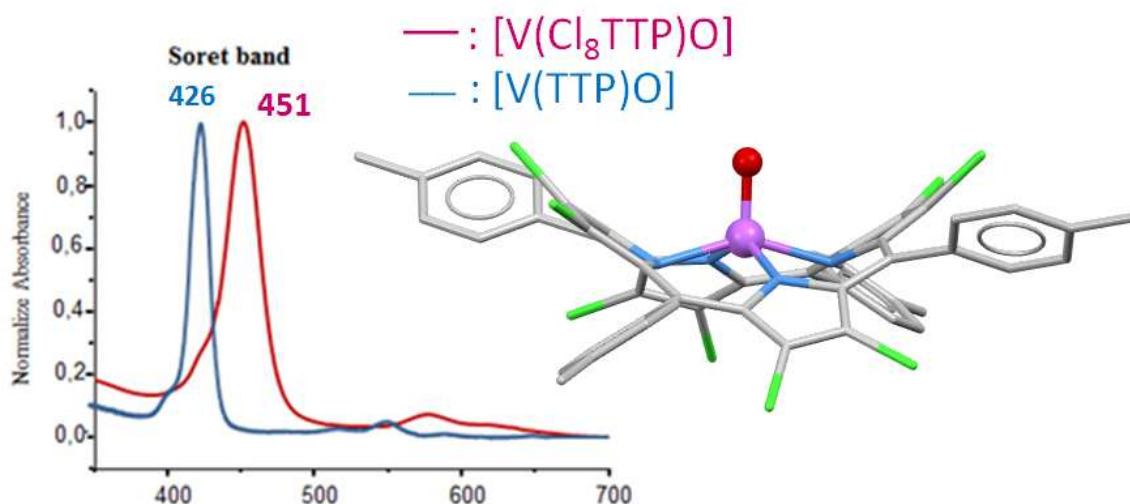
The (Oxo)(2,3,7,8,12,13,17,18-Octachloro-5,10,15,20-Tetrakis(4-tolylporphyrinato)]Vanadium(IV) : Synthesis, UV-visible, Cyclic Voltammetry and X-Ray Crystal Structure

Chadlia Mchiri[a], Nesrine Amiri[a], Souhir Jabli[a], Thierry Roisnel[b], Habib Nasri[a]*

[a]*Laboratoire de Physico-chimie des Matériaux, Faculté des Sciences de Monastir, Avenue de l'environnement, 5019 Monastir, University of Monastir, Tunisia.*
[b]*Centre de Diffractométrie X, Institut des Sciences Chimiques de Rennes, UMR 6226, CNRS–Université de Rennes,1,Campus de Beaulieu, 35042 Rennes Cedex,*
France.

Abstract

The present work is concerned with the oxo vanadium(IV) complex of 2,3,7,8,12,13,17,18-octachloro-5,10,15,20-tetrakis(4-tolylporphyrin) with the formula [V(Cl$_8$TTP)O] (**I**), which was prepared by reacting the oxo[5,10,15,20-tetrakis(4-tolylporphyrinato)]vanadium(IV) complex ([V(TTP)O]), under aerobic atmosphere, with a large excess of thionyl chloride (SOCl$_2$). The title compound was characterized by UV-visible spectroscopy, cyclic voltammetry and X-ray crystal structure. The electron-withdrawing chlorine substituents at the pyrrole carbons in the vanadyl-Cl$_8$TTP derivative produce remarkable redshifts of the Soret and Q absorption bands and an important anodic shift of the porphyrin ring oxidation and reduction potentials. This is an indication that the porphyrin core of complex (**I**) is severely nonplanar in solution. The molecular structure of our vanadyl derivative shows a very high *saddle* distortion and an important *ruffled* deformation of the porphyrin macrocycle. The crystal structure of (**I**) is made by one-dimensional chains parallel to the *c* axis where channels are located between these chains.

1. Introduction

The β-pyrrole positions halogenated porphyrins and metalloporphyrins were studied as early as 1973 when Callot prepared several β-pyrrole bromine free bases porphyrins and nickel metalloporphyrins [1]. Free bases and metallated *meso*-arylporphyrins are widely used in porphyrin and metalloporphyrins chemistry because of their usually easy preparation.

---

* Corresponding author. Fax: +216 73 500 278.
E-mail address: hnasri1@gmail.com or Habib.Nasri@fsm.rnu.tn (H. Nasri).

However, the phenyl groups and the porphyrin core are sterically constrained to lay essentially perpendicular to each other, therefore, only the inductive effect of the phenyl is transmitted to the porphyrin core. The substitution at the β-pyrrole positions of the porphyrin with electron donor/withdrawing groups can have a direct effect on the electronic properties of these species since they case undergo direct conjugation of the porphyrin π system. About ten years after the first preparation by Callot of several β-pyrrole brominated porphyrins and metalloporphyrins, these halogenated porphyrin species were successfully used for catalytic alkane hydroxylation and olefin epoxidation [2,3]. For these derivatives, the electron-withdrawing substituents at the β-pyrrole positions increase the catalytic activity of these species and makes these compounds robust and highly efficient oxygen transfer catalysts. It has been shown that the presence of eight halogens at the β-pyrrole positions results in the severe *saddle* and moderate *ruffling* distortions of the porphyrin core due to the strong steric interaction between the halogens at the β-pyrrole positions and the *meso*-phenyls [4]. As a consequence, the electronic spectra of these species exhibit important redshift of the Soret and Q bands. Additionally, the cyclic voltammograms of these β-pyrrole halogenated porphyrin species present a large anodic shift of the redox potentials of the porphyrin ring compared to the unsubstituted *meso*-porphyrins derivatives [5]. In 2011, Taghavi *et al.*, [6] reported the catalytic activity of the high-valent bis-(trifluoromethanesulfonato) [tetraphenylporphyrinato]vanadium(IV)] ([V(TPP)(Otf)$_2$]) in the acetylation of alcohols and phenols with Ac$_2$O. By the other hand, it is noteworthy that several vanadyl porphyrin complexes present interesting anti-HIV properties towards infected immortalized T-cells [7]. With the aim of understanding the effect of the presence of chlorine atoms on the β-pyrrole positions on the electronic and structural properties of vanadyl metalloporphyrins, we report here the preparation of the oxo β-pyrrole octachlorinated porphyrin vanadyl complex namely oxo[(2,3,7,8,12,13,17,18-octachloro-5,10,15,20-tetrakis(4-tolylporphyrinato)] vanadium(IV) [V(Cl$_8$TTP)O] (**I**) using a relatively easy synthetic procedure involving the reaction of the vanadyl complex with the unsubstituted *meso*-tertakis(4-tolylporphyrin) ([V(TTP)O]) with an excess of thionyl chloride. This coordination complex was characterized with UV-visible spectroscopy, cyclic voltammetry and X-ray molecular structure.

2.1 General Information

All solvents and reagents were purchased from commercial supplies and used without further purifications. The [VO(TTP)] starting material were synthesized according to the standard literature method **[8]**. All manipulations were carried out under aerobic conditions. The UV-visible spectra were recorded with a WinASPECT PLUS (validation for SPECORD PLUS version 4.2) scanning spectrophotometer. MALDI-TOF MS spectra were recorded on an Ultraflex mass spectrometer (Bruker Daltonics) without a matrix. Cyclic voltammetry (CV) experiments were performed with a CH-660B potentiostat (CH Instruments). All analytical experiments were conducted at room temperature under an argon atmosphere (argon stream) in a standard one-compartment, three-electrode electrochemical cell. Tetra-n-butylammonium hexafluorophosphate (TBAPF$_6$) was used as the supporting electrolyte (0.1 M) in dichloromethane previously distilled over calcium hydride under argon. An automatic Ohmic drop compensation procedure was systematically implemented before the CV data were recorded with electrolytic solutions containing the studied compounds at concentrations of ca. 10^{-3} M. CH Instruments vitreous carbon (ϕ= 3 mm) working electrodes were polished with 1 μm diamond paste before each recording. The saturated calomel electrode SCE (TBAPF$_6$ 0.1 M in CH$_2$Cl$_2$) redox couple was used as the reference electrode. The potential of the ferrocene/ ferrocenium redox couple was used as an internal reference (0.37 V/SCE experimental conditions).

*2.2 Synthesis of the oxo[(2,3,7,8,12,13,17,18-octachloro-5,10,15,20-tetrakis(4-tolylporphyrinato)]vanadium(IV) [V(Cl$_8$TTP)O] (**I**)*

[V(TTP)O] (100 mg, 0.135 mmol) and SOCl$_2$ (1 mL, 13.75 mmol) were stirred together in dichloromethane (10 mL) at room temperature for two hours. The color of the solution changes from purple to green corresponding to complex (**I**) and the solvents was removed under vacuum. Crystals of (**I**) were obtained by slow diffusion of n-hexane unto the chloroform solution (109 mg, yield ~ 80%).

Anal. Calc. for (**1**), C$_{48}$H$_{28}$Cl$_8$N$_4$OV (1011,34 g/mol): C, 57.01; H, 2.79; N, 5.54%. Found: C, 57.12; H, 2.81; N, 5.67%. UV-visible [λ$_{max}$ (nm) in CH$_2$Cl$_2$, (ε.10^{-3} L.mol^{-1}.cm^{-1})]:451 (398), 577 (5.1); ^{1}H NMR (300 MHz, CDCl$_3$, 298 K): δ(ppm): 8.04 (d, 8H, Ho,o'), 7.72 (d, 8H, Hm,m'), 2.69 (s, 12H, -CH$_3$).MS (MALDI-TOF) *m/z* = 1012.33 [V(Cl$_8$TTP)O]+H]$^+$.

2.3 X-Ray Structural Analysis

A suitable crystal of (**I**) with approximate dimensions 0.31x0.26x0.15 mm^3 was selected and mounted on a glass fiber oil on a D8 VENTURE Bruker AXS diffractometer equipped with a graphite monochromatic Mo-K radiation source (λ = 0.71073 Å). The unit-cell parameters were calculated and refined from the full data and the data collection was performed with a Bruker D8 VENTURE diffractometer at 150 K. The reflections were scaled and corrected for absorption effects by using SADABS **[9]**. The structure was solved by direct method by using SIR-2004 program **[10]** and refined by full-matrix least-squares techniques on F^2 by using the SHELXL-97 program **[11]**. The crystallographic data and structural refinement details of complex (**I**) are shown in Table 1.

Table 1. Crystal data and structural refinement for [V(Cl$_8$TTP)O] complex (**I**).

Formula	C$_{48}$H$_{28}$Cl$_8$N4OV
D$_{calc}$./ g cm^{-3}	1.633
μ/ mm^{-1}	0.807
Formula Weight	1011.28
Color	black
Shape	prism
Size/mm^3	$0.31 \times 0.26 \times 0.15$
T(K)	150
Crystal System	tetragonal
Space Group	*I 4$_1$/a*
a (Å)	20.4557(9)
b (Å)	20.4557(9)
c (Å)	9.8334(6)
V(Å^3)	4114.7(6)
Z	4
θ_{min} (°)	3.04
θ_{max} (°)	26.00
Reflections measured	10240
Reflections used	2004
R$_{int}$	0.0518
Parameters	146
Largest Peak Largest Peak	0.554
Deepest Hole	-1.759
S [Goodness of fit]	1.136
R_1[a], wR$_2$[b] [F$_o$ > 4σ(F$_o$)]	R_1 = 0.0791, wR_2 = 0.2476
R_1[a], wR$_2$[b][all data]	R_1 = 0.0902, wR_2 = 0.2581
CCDC	1532095

[a]: $R_1 = \Sigma||F_O| - |F_C||/\Sigma|F_O|$. [b]: $wR_2 = \{\Sigma[w(|F_O|^2 - |F_C|^2)^2]/\Sigma[w(|F_O|^2)^2]\}^{1/2}$.

3. Results and discussion

3.1. Synthesis

In 1973 Callot *et al.*, [1] reported for the first time the β-pyrrole halogenation reactions on the *meso*-tetraphenylporphyrin (H$_2$TPP). The author was able to substitute up to four bromine at the β-pyrrole positions by reaction the H$_2$TPP porphyrin with increasing amounts of N-bromosuccinimide (NSB) in chloroform under reflux. Later on, Krishnan *et al.*, [12] have prepared the 2,3,7,8,12,13,17,18-octabromo-*meso*-tetraphenylporphyrin (H$_2$Br$_8$TPP) by reacting the [Cu(TPP)] complex with an excess of liquid bromine leading to the β-pyrrole octabromo derivative [Cu(Br$_8$TPP)]. The free base H$_2$Br$_8$TPP was then obtained by demetallation using perchloric acid. Meunier *et al.* [13] used also an indirect method to prepare the 2,3,7,8,12,13,17,18-octabromo-*meso*-tetratetramesitylporphyrin H$_2$Br$_8$TMP starting from the [Zn(Br$_8$TMP)] complex which is demetallated using the trifluoacetic acid (CF$_3$COOH).

A new synthetic method, which is easier and give a better yield than those mentioned above, was reported by Mironov *et al.,* [14] for the preparation of the octachloro β-pyrrole porphyrin complexes which were synthetized starting from the desired metallated unsubstituted porphyrin type [M(*meso*-Porph)] using the thionyl chloride SOCl$_2$ as reagent and solvent.

In the literature, the only reported vanadyl-porphyrin complex with a β-pyrrole octachlorinated porphyrin is the [V(Cl$_8$TPP)O] for which only a communication of the molecular structure of this species is reported [15]. We used a modified Mironov synthetic method [14] to prepare the vanadyl-Cl$_8$TTP complex (**I**) starting from the oxo(5,10,15,20-[tetrakis(4-tolylporphyrinato]vanadium(IV) complex ([V(TTP)O]) for which we added an excess of SOCl$_2$ under room temperature leading after about 2 hours to a green solution of complex (**I**) namely : the oxo[(2,3,7,8,12,13,17,18-octachloro-5,10,15,20-tetrakis(4-tolylporphyrinato)]vanadium(IV) with the formula [V(Cl$_8$TTP)O]. Our synthetic vanadyl species (**I**) was obtained with a high yield of about 80%.

3.2. Solution UV-vis investigation

Ghos *et al.*, [16] indicated that the porphyrin-central metal interactions « porphyrin(a$_{2u}$)-metal(d$_{xy}$) » and « porphyrin(a$_{2u}$)-metal ($d_{x^2-y^2}$) » in a D$_{4h}$ symmetry exist in *ruffl*e and

saddle distortions respectively but cannot occur in planar porphyrin macrocycle systems. This is due to the fact that in planar porphyrins, the HOMO a_{1u} and a_{2u} orbitals and the d_{xy} and $d_{x^2-y^2}$ metal orbitals are orthogonal. Therefore, the HOMO orbital of the porphyrin complex is destabilized, while the LUMO orbital of the metalloporphyrin is practically unchanged, leading to a decrease of the HOMO-LUMO energy. Consequently, the Soret and the Q absorption bands are redshifted. Additionally, back to 1973, Callot pointed out that for β-pyrrole substituted porphyrin, each bromine substitution at the pyrrole position contributed a redshift of about 6 nm with respected to the unsubstituted H_2TPP porphyrin [17,19]. In Table 2 are reported the UV-visible data of several metalloporphyrins with β-pyrrole halogenated porphyrins. All these species present very redshifted Soret and Q bands. The absorption spectra of (**I**) and the [VO(TTP)] starting material are shown in Figure 1. The Soret band value of the [V(TTP)O] starting material with the unsubstituted TTP porphyrinate, which is 426 nm, shifts to 451 nm after adding a large excess of $SOCl_2$ in the dichloromethane solvent leading to the [V(Cl_8TPP)O] complex (**I**) with the β-pyrrole chlorinated Cl_8TTP porphyrinate and the color of the solution changes from purple (TTP-vanadyl derivative) to green (Cl_8TTP-vanadyl species). We notice that the values of λ_{max} of the Soret and Q bands of (**I**) are quite smaller than that of the β-pyrrole brominated Br_8TPP derivative [V(Br_8TPP)O] [12] (which is 464 nm) .These results cannot be explained only by the withdrawing effect of the chlorine atoms at the β-positions of the porphyrin. The important red shift of the Soret and Q bands is mainly due to the bulkiness of the β-pyrrole groups which lead to an important steric interaction between these groups and the phenyls at the *meso* positions of the porphyrin. Additionally, the fact that the electronic spectrum of (**I**) is very redshifted is an indication that in solution, this derivative and the related halogenatedspecies present very *saddle* and *ruffed* deformations of the porphyrin macrocycles.
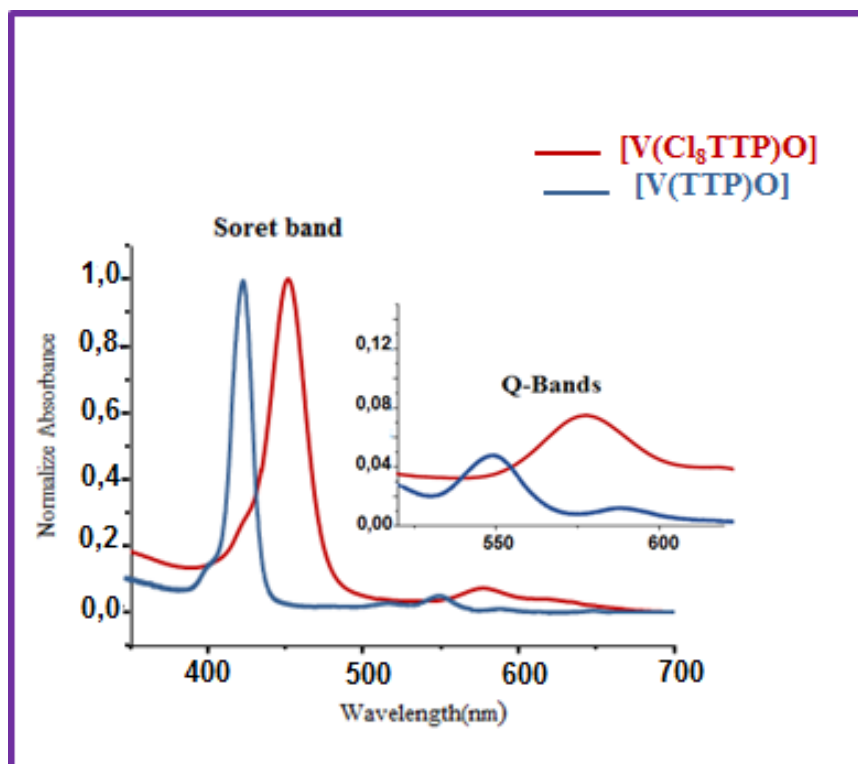
Figure 1. UV-visible absorption spectra of the starting material [V(TTP)O] and [V(Cl$_8$TTP)O] (**I**) in CH$_2$Cl$_2$ solution at concentrations ~10^{-5}. The inset shows enlarged view of the Q bands.

Table 2. UV−visible data for [V(Cl$_8$TTP)O] (**I**) and selected β-pyrrole halogenated porphyrin complexes.

Complex	Solvent	Soret band	Q bands		Ref.
		λ_{max} [nm] ($\varepsilon.10^{-3}$ L.mol^{-1}.cm^{-1})			
[Ni(Cl$_8$TPP)][a]	CH$_2$Cl$_2$	**439** (468)	553 (1.10)	587	[20]
[Ni(Br$_8$TPP)][b]	CH$_2$Cl$_2$	**449** (557)	561 (1.20)	599	[20]
[Ni(Cl$_8$TBPP)][c]	n-hexane	**456**	584	652	[14]
[Ni[I$_8$TpCF$_3$PP][d]	CH$_2$Cl$_2$	**465** (161.3)	578 (17.8)	615(11.8)	[21]
[ZnI$_8$TpCF$_3$PP][d]	CH$_2$Cl$_2$	**495** (110.2)	633 (11.4)	680(12.3)	[21]
[Zn (Cl$_8$TFPP)][e]	CH$_2$Cl$_2$	**442**	575	-	[22]
[Zn^{II}(Br$_8$TPP)][b]	CH$_2$Cl$_2$	**466** (257)	598 (14.0)	656 (12.3)	[12]
[Co^{III}(Br$_8$TPP)][b]	PhCN	**480** (81.6)	590 (8.6)	637 (5.9)	[23]
[Co^{II}(Br$_8$TPP)][b]	PhCN	**458** (80.3)	568 (10.3)	-	[23]
[Cu(Cl$_8$TBPP)][c]	n-hexane	**463**	588	660	[14]
[Cu^{II}(Br$_8$(TPP)][b]	CH$_2$Cl$_2$	**466** (132)	581 (18)	-	[12]
[CuI$_8$TpCF$_3$PP][d]	CH$_2$Cl$_2$	**486** (96.4)	599(75.4)		[21]
[Ru(Br$_8$TMP)(O)$_2$][f]	CH$_2$Cl$_2$	**456** (398.1)	540(21.9)		[24]
[Fe^{II}(Cl$_8$TPP)Cl][a]	PhCN	**468** (160)	-	590	[25]
[Pd(Cl$_8$TBPP)][c]	n-hexane	**436**	567	642	[14]
[Tb^{III}(Cl$_8$TPP)(OAc)][a,g]	CH$_2$Cl$_2$	**460** (59)	553 (5)	598 (8)	[20]
[Tb^{III}(Br$_8$TPP)(OAc)][b,g]	CH$_2$Cl$_2$	**474** (45)	552 (3.0)	612 (2.9)	[20]

[V(TTP)O][h]	CH_2Cl_2	**426**	548	-	this work
[V(Br$_8$TPP)O][b]	CH_2Cl_2	**464** (229)	589 (17.8)	-	**[12]**
[V(Cl$_8$TTP)O]	CH_2Cl_2	**451** (398)	577 (5.1)	-	this work

[a]:Cl$_8$TPP = 2,3,7,8,12,13,17,18-octachloro-5,10,15,20-tetraphenylporphyrinato,
[b]: Br$_8$TPP = 2,3,7,8,12,13,17,18-octabromo-5,10,15,20-tetraphenylporphyrinato,
[c]: Cl$_8$TBPP = 2,3,7,8,12,13,17,18-octachloro-5,10,15,20-tetrakis(3,5-di-*tert*butylphenyl)porphyrinato,
[d]:I$_8$TpCF$_3$PP =2,3,7,8,12,13,17,18octaiodo5,10,15,20tetrakis[4(trifluoromethyl)phenyl]porphyrinato,
[e]: Cl$_8$TFPP =2,3,7,8,12,13,17,18-octachloro-5,10,15,20-tetrakis(pentafluorophenyl)porphyrinato,
[f]: Br$_8$TMP = 2,3,7,8,12,13,17,18-octabromo-5,10,15,20-tetramesitylporphyrinato,
[g]: OAc = acetate, [h]:TTP = 5,10,15,20-tetratoloylphenylporphyrinato,

3.3 Cyclic Voltammetry

The electrochemical behavior of complex (**I**) was studied by cyclic voltammetry (CV) with the tetra-n-butylammonium hexafluorophosphate (TBAPF$_6$) as the supporting electrolyte (0.1 M) in the non-coordinating solvent CH_2Cl_2 under an argon atmosphere. The voltammogram of our vanadyl species [V(Cl$_8$TTPO] (**I**) is depicted in Figure 2 and the electrochemical of (**I**) and several related species are collected in Table 3. It has been shown that the presence of electron-withdrawing halogen group (such as chloro and bromo) in the β-pyrrole positions of a porphyrin decreases the electron density at the porphyrin macrocycle which causes an anodic shift in the ring oxidation and reduction potentials of the porphyrins **[26]**. By the other hand, several investigations **[27,28]** show that the presence of bulky substituents such as bromine and chlorine at the β-positions of the porphyrin causes an important deformation of the porphyrin core (especially the *saddle* distortion) which increases the half wave potential values of the oxidation and especially the reduction of the porphyrin ring. Therefore, both induction withdrawing effect and steric hindrance effects of the β-pyrrole halogenated porphyrins and metalloporphyrins have an important effect on the electrochemical and UV-visible data of these species. Consequently, these two effects induce a destabilization of the HOMO orbitals, leaving the LUMO orbitals relatively unchanged (slight stabilization) **[20]**. As shown in Table 3, the β-pyrrole octachloro and the octabromo porphyrins (H$_2$Cl$_8$TPP and H$_2$Br$_8$TPP) are easier to reduce and harder to oxidize compared to the unsubstituted *meso*-tetraphenylporphyrin H$_2$TPP because of the important electron deficient character of the halogenated porphyrins. Indeed, the half potential values of the first and second oxidations are 1.02 V / 1.26 V, 1.04 V / 1.26 V and 1.03 V / 1.65 V for the H$_2$TPP, H$_2$Cl$_8$TPP and H$_2$Br$_8$TPP respectively while the first and second reductions values are -1.20 V / -1.55 V, -0.83 V / -1.11 V and -0.61 V / -0.97 V for the H$_2$TPP unsubstituted porphyrin, the octachloro porphyrin and the octabromo porphyrin respectively

[29]. For the vanadyl species, we observe the same trend than that of the free bases. Thus, the $E_{1/2}$ values of the oxidation and the reduction waves increase from the TPP-vanadyl **[12]** to the Cl_8TTP-vanadyl and the Br_8TPP-vanadyl (Table 3). We noticed that the oxidation and reduction potentials values of the free bases H_2TPP, H_2Cl_8TTP and H_2Br_8TPP are shifted to more positive values compared to the corresponding vanadyl $[V(TPP)O]$, $[V(Cl_8TTP)O]$ and $[V(Br_8TPP)O]$ complexes. The porphyrin HOMO–LUMO gap value can be expressed as the potential difference between the value of the first oxidation half potential and the value of the first reduction potential wave. As mentioned above, the β-pyrrole halogenated porphyrin **[20]** and the corresponding vanadyl species (**I**) present smaller Gap values than the H_2TPP porphyrin **[29]** and the $[V(TPP)O]$ species **[30]** with the values 2.22 eV / 2.40 eV for H_2TPP / $[V(TPP)O]$ and 1.87 eV / 2.04 eV for H_2Cl_8TPP / $[V(Cl_8TTP)O]$ (Table 3).
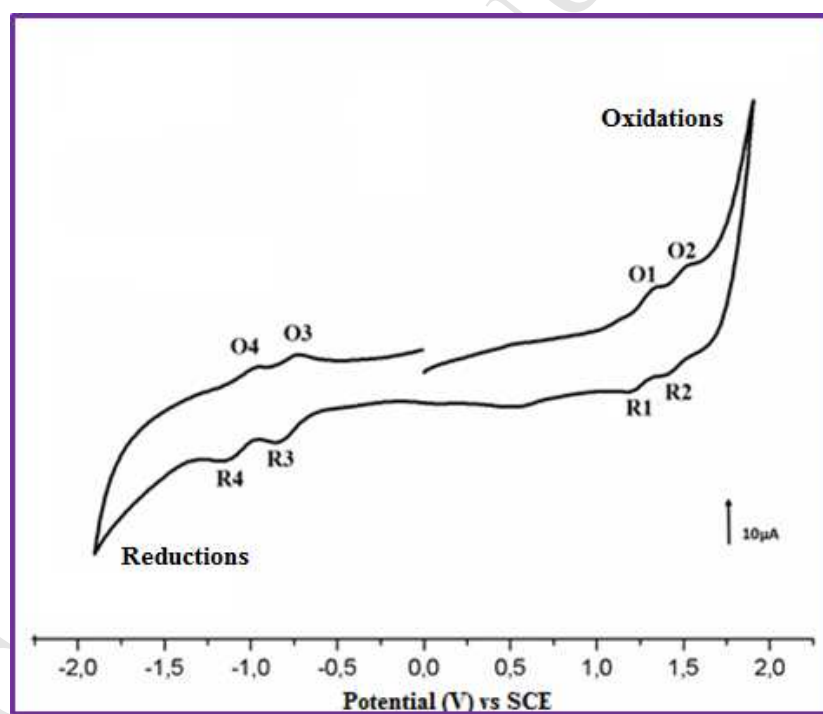

Figure 2. Cyclic voltammogram of $[V(Cl_8TTP)O]$ (**I**). The solvent is CH_2Cl_2, the concentration is ca. 10^{-3} M in 0.2 M $TBAPF_6$, the scan rate is 100 mV/s, vitreous carbon working electrode ($\emptyset = 3$ mm).

Table 3. Half-wave potentials (in V vs SCE)[a] of several *meso*-porphyrins, complex **(I)** and a selection of V(IV) metalloporphyrins.

Complex	Ring oxidations		Ring reductions			Ref.
	1st oxidation (O1/R1)	2nd oxidation (O2/R2)	1st reduction (R3/O3)	2nd reduction (R4/O4)	HOMO-LUMO Gap[b] (eV)	
H$_2$TPP[c]	1.02	1.26	-1.20	-1.55	2.22	**[29]**
H$_2$Cl$_8$TPP[d]	1.04	1.26	-0.83	-1.11	1.87	**[20]**
H$_2$Br$_8$TPP[e]	1.03	1.65	-0.61	-0.97	-1.64	**[20]**
[V(TPP)O]	1.35	1.13	-1.13	-1.51	2.48	**[30]**
[V(Cl$_8$TTP)O]	1.25	1.46	-0.79	-1.06	2.04	this work
[V(Br$_8$TPP)O]	1.38	1.54	-0.54	-0.78	1.92	**[12]**

[a]: the solvent used is the dichloromethane, [b]: HOMO-LUMO Gap = $E_{1/2}$(O1) - $E_{1/2}$(R3), [c]: H$_2$TPP = 5,10,15,20-tetraphenylporphyrin, [d]: H$_2$Cl$_8$TPP = 2,3,7,8,12,13,17,18-octachloro-5,10,15,20-tetraphenylporphyrin, [e]: H$_2$Br$_8$TPP = 2,3,7,8,12,13,17,18-octabromo-5,10,15,20-tetraphenylporphyrin.

3.4 X-ray Structural properties of [V(Cl₈TTP)O] (I)

Complex (**I**) crystallizes in the tetragonal crystal system (space group *I4₁/a*) and the asymmetric unit contains one quarter of the [V(Cl₈TTP)O] complex where the vanadium central metal and the oxygen atom of the oxo axial ligand lie in a fourfold rotoinversion axis. The V(IV) cation is chelated by four pyrrole N atoms of the porphyrinate anion and coordinated by the oxygen atom of the oxo axial ligand. Nevertheless, the vanadyl group (V=O) is disordered in two positions with 0.5/0.5 occupancy ratio required by the rotoinversion symmetry. The ORTP diagram of (**I**) is illustrated in Figure 3.
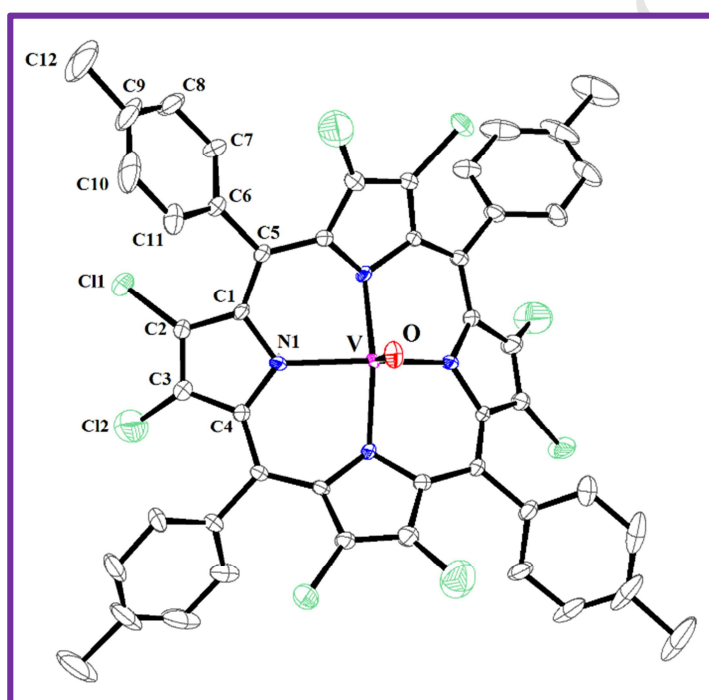

Figure 3. ORTP diagram of [VO(Cl₈TTP)] (**I**). Ellipsoids are drawn at the 50% probability level.

The porphyrin core presents essentially four major deformations **[31]** namely: (i), the *doming* distortion (*dom*) is often observed in five-coordinated porphyrin complexes when the axial ligand causes a displacement of the metal ion out of the mean plane and the nitrogen atoms are also displaced toward the axial ligand, (ii) the *waving* distortion (*wav*) where the four fragments «(β-carbon)-(α-carbon)-(*meso*-carbon)-(α-carbon)-(β-carbon)» (or C_β-C_α-C_m-$C_{\alpha'}$-$C_{\beta'}$) (Figure 4) are alternatively above and below the mean plan of porphyrin (P_C plane), (iii) the *ruffling* distortion (*ruff*) is indicated by the values of the *meso*-carbon atoms above and below the porphyrin mean plane and (iv) the *saddle* distortion (*sad*)

involves the displacements of the pyrrole rings alternately above and below the mean porphyrin macrocycle so that the pyrrole nitrogen atoms are out of the mean plane. The *saddle* deformation can also be defined by the dihedral angle δ<(Pyr/Pyr)> between adjacent and opposite pyrrole rings [19]. The most important feature of the structure of our vanadyl derivative [V(Cl$_8$TPP)O] (**I**) is the very important distortion of the porphyrin macrocycle. Indeed, the three different views of Figure 5 show how important are the *saddle* and *ruffling* deformations of the porphyrin cycle of (**I**). By the other hand, Figure 4 illustrates the formal diagram of the porphyrin macrocycle of (**I**) showing the displacements of each atom from the mean plane of the 24-atom porphyrin core in units of 0.01 Å. As shown by the very high values of the displacement of the pyrrole and *meso* atoms from the 24-atoms mean plane, the porphyrin core of (**I**) presents very high *saddle* and an important *ruffling* deformations.
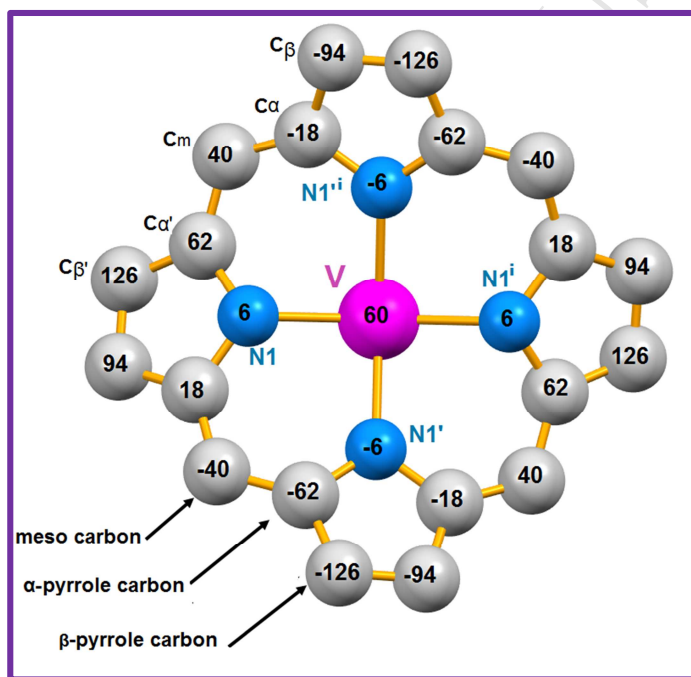

Figure 4. Formal diagrams of the porphyrinato cores of (**I**). The displacement of each atom from the mean of the 24-atom porphyrin macrocycle in given in unit of 0.01 Å.
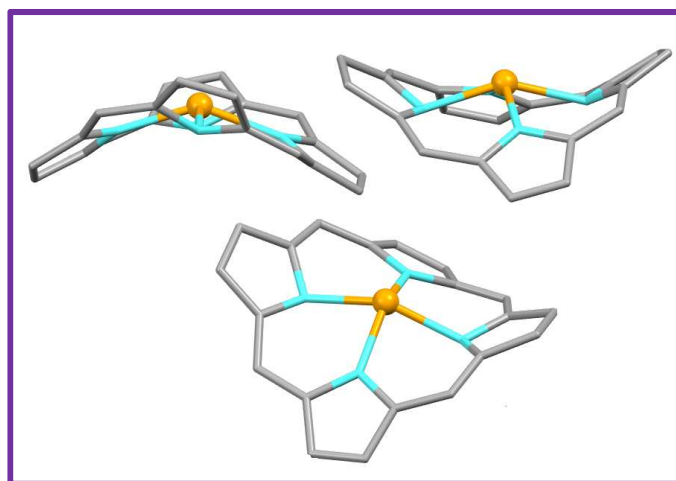
Figure 5. Schematic representations showing the porphyrin core deformations of (**I**).

With the aim to see the effect of the β-pyrrole substitutions on the deformations of the porphyrin core, several examples of metalloporphyrins, where the β-positions of the porphyrins are occupied by halogens are reported in Table 4. Indeed, in the case of zin(II) porphyrins, the average value of the dihedral angle between two adjacent pyrroles (δ<Pyr/Pyr>) for the *meso*-tetraphenylporphyrin derivative [Zn(TPP)] **[32]** is equal to 3.94°. The effect of presence of a bromine atoms in the β-pyrrole positions leads to a significant increase of the *saddle* deformation, e.g., for the [Zn(Br$_8$TPP)(NC-Bu)$_2$] complex (Br$_8$TPP is the β-halogenated porphyrin: 2,3,7,8,12,13,17,18-octachloro-*meso*-tetraphenylporphyrinato) the δ<Pyr/Py> angle value is 34.70° **[33]**.

Table 4. Selected structural features of several metalloporphyrins.

Complex	M−N$_P$^{a} (Å)	M−P$_C$^{b}(Å)	δ<(Pyr/Pyr)>(°)^c	Δ<(Ph/P$_C$)> (°)^d	Ref.
[Zn(TPP)]^e	2.038	0.000	3.94	68.07	**[32]**
[Zn(Br$_8$TPP)(NC-Bu)$_2$]^{f,g}	2.027	0.053	34.70	56.88	**[33]**
[Zn^{II}(Cl$_8$TPFPP)]^h	2.033	0.00	25.44	58.77	**[34]**
[Zn^{II}(Br$_8$TPFPP)]^i	2.04(2)	0.174	31.31	54.74	**[35]**
[Zn^{II}(I$_8$TpCF$_3$PP)]^j	2.056(5)	0.311	40.24	8.18	**[21]**
[Ni(TPP)]^e	1.947	0.000	24.29	78.7	**[36]**
[Ni(Cl$_8$TPP)]^k	1.907(3)	0.000	38.37	56.81	**[14]**
[Ni(Br$_8$TPFPP)]^i	1.9(1)	0.017	38.93	45.13	**[36]**
[Fe^{II}(Cl$_8$TPFPP)(L)$_2$]^{h,l}	1.981(5)	0.037	28.76	59.87	**[37]**
[Fe^{II}(Br$_8$TPFPP)Cl]^i	2.06(1)	0.469	39.07	47.53	**[38]**
[V(TPP)O]^e	2.080(6)	0.53	0.00	90	**[39]**
[V(Cl$_8$TPP)O]^k	2.056(8)	0.518	25.36	62.15	**[16]**
[V(Cl$_8$TTP)O]	2.047(4)	0.581	44.16	33.19	This work
[V(TTP)(Cl)(THF)]^n	2.057	0.000	2.34	74.45	**[40]**

_____

[a]: M—N_P = average equatorial Mn—Npyrrole bond length.

[b]: M—P_C= displacement of the metal atom from the 24 atoms mean plan of the porphyrin core (P_C).

[c]:δ<(Pyr/Pyr)> = the dihedral angle between two adjacent pyrrole rings.

[d]:Δ<(Ph/PC)> = average value of the dihedral angles between the Pc plane and the phenyl ring.

[e]: TPP = 5,10,15,20-tetraphenylporphyrinato,

[f]:Br_8TPP = 2,3,7,8,12,13,17,18-octabromo-5,10,15,20-tetraphenylporphyrinato,

[g]:NC-Bu = butyronitrilo-N,

[h]:Cl_8TPFPP = tetrakis(pentafluorophenyl)-2,3,7,8,12,13,17,18-octachloroporphyrinato,

[i]:Br_8TPFPP = tetrakis(pentafluorophenyl)-2,3,7,8,12,13,17,18-octabromoporphyrinato,

[j]: I_8TpCF$_3$PP = 2,3,7,8,12,13,17,18-octaiodo-5,10,15,20-tetrakis(4-(trifluoromethyl)phenyl)porphyrinato,

[k]:Cl_8TPP = 2,3,7,8,12,13,17,18-octachloro-5,10,15,20-tetraphenylporphyrinato,

[l]: L = 1-MeIm = 1-methyl imidazole,

[n]: TTP = 5,10,15,20-tetratoloylphenylporphyrinato.

The *saddle* distortion is also characterized by the average values of the four dihedral angles between the P_C mean plan and the phenyl groups of the porphyrin [Δ<(Ph/P_C)>] [41]. For *meso*-arylporphyrin derivatives with important *saddle* deformation, the phenyl rings rotate toward the porphyrin core (P_C) to minimize the steric interaction with the β-pyrrole substituents. As shown in Table 4, for the vanadyl derivative with the unsubstituted TPP porphyrin ([V(TPP)O]), the Δ<(Ph/P_C)> value is 90° while for the octachloro vanadyl-Cl_8TPP and vanadyl-Cl_8TTP, the Δ<(Ph/P_C)> values are 62.15° and 33.16° respectively. We noticed that the Δ<(Ph/P_C)> angle values decrease from [V(TPP)O] (Δ= 90°) then [V(Cl_8TPP)O] (Δ= 62.15°) and then our synthetic vanadyl-TCl8TTP species with a Δ<(Ph/P_C)> value of 33.19°. These δ<(Pyr/Pyr)> and Δ<(Ph/P_C)> dihedral angle values of complex (**I**) is a clear indication that our vanadyl-Cl_8TTP derivative exhibits the highest *saddle* deformation compared to the other vanadyl metalloporphyrins. One can wonder why the vanadyl-Cl_8TTP species (**I**) exhibits higher *saddle* deformation than the related vanadyl-TPP derivative. This could be explained by the methyl group in the *para* positions of the phenyl rings of the TTP porphyrinato ligand which increases the steric interactions with the chlorine atoms in the β-pyrrole positions. The V=O distance value of our derivative is 1.604 (10) Å which is in the range [1.546 Å-1.697] Å (Table 4) of vanadium(IV) metalloporphyri [42,43]. Notably, for the unsibstitued TPP derivative [V(TPP)O [39], the V=O bond lengh is 1.625 (16) Å which is relaively close to our Cl_8TTP-vanadyl species [1.604 (10) Å] indicating that the porphyrin core deformations have only small effect upon the Lewis acidity of the vanadium(IV) metal center. For complex (**I**), the average equatorial distance between the vanadium center metal and the four nitrogens of the pyrrole ring (V—Np) is 2.047(4) which is also in the range of known vanadium(IV) metallaporphyrins (Table 4). This indicates that the deformations of the porphyrin core have also small effect on the

V−Np bond lengths. The crystal structure of (**I**) features one-dimensional chains along the [100] direction. Within one chain, the [V(Cl$_8$TTP)O] molecules are sustained together with weak C−H⋯O non-conventional hydrogen bonds between the carbon C12 of the methyl group of one Cl$_8$TTP porphyrin and the oxygen O1 of the vanadyl group and an adjacent [V(Cl$_8$TTP)O] molecule and between the C8 carbon of a phenyl ring of one TCl$_8$PP moiety and the oxo ligand of a neighboring [V(Cl$_8$TPP)O] species (Figure 6, Table 5). These chains are linked together via the C−H⋯Cl2 hydrogen bond between the carbon C12 of the methyl group of a phenyl ring of one [V(Cl$_8$PP)O] molecule of one chain and the chlorine atom Cl2 of an adjacent [V(Cl$_8$TPP)O] molecule of the nearby chain (Figure SI-1 as supplementary information, Table 5). It is noteworthy the presence of channels with a radius of about 5.5 Å parallel to the *c* axis between the one-dimensional chains (Figure 7).
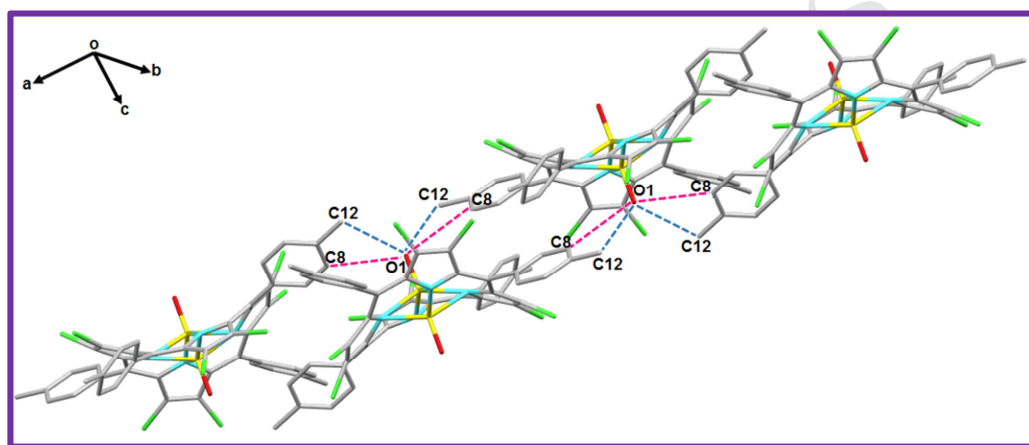

Figure 6. A partial view of the crystal packing of (**I**) showing the links within one layer between the [V(Cl$_8$TTP)O] complexes via non-classical C—H⋯O hydrogen bond.

Table 6. Hydrogen bonds and selected C–H⋯X intermolecular interactions for complex (**I**).

D−H⋯A[a]	Symmetry of A	D[a]⋯A[b] [Å]	D–H⋯A [°]	D⋯A [Å]
C8−H8⋯O1	1/4+y,1/4-x,1/4+z	3.386(7)	152	2.54
C12−H12A⋯O1	3/4-y,1/4+x,1/4+z	3.338(11)	161	2.42
C12−H12B⋯Cl2	1/4+y,3/4-x,3/4-z	3.310(10)	130	2.61

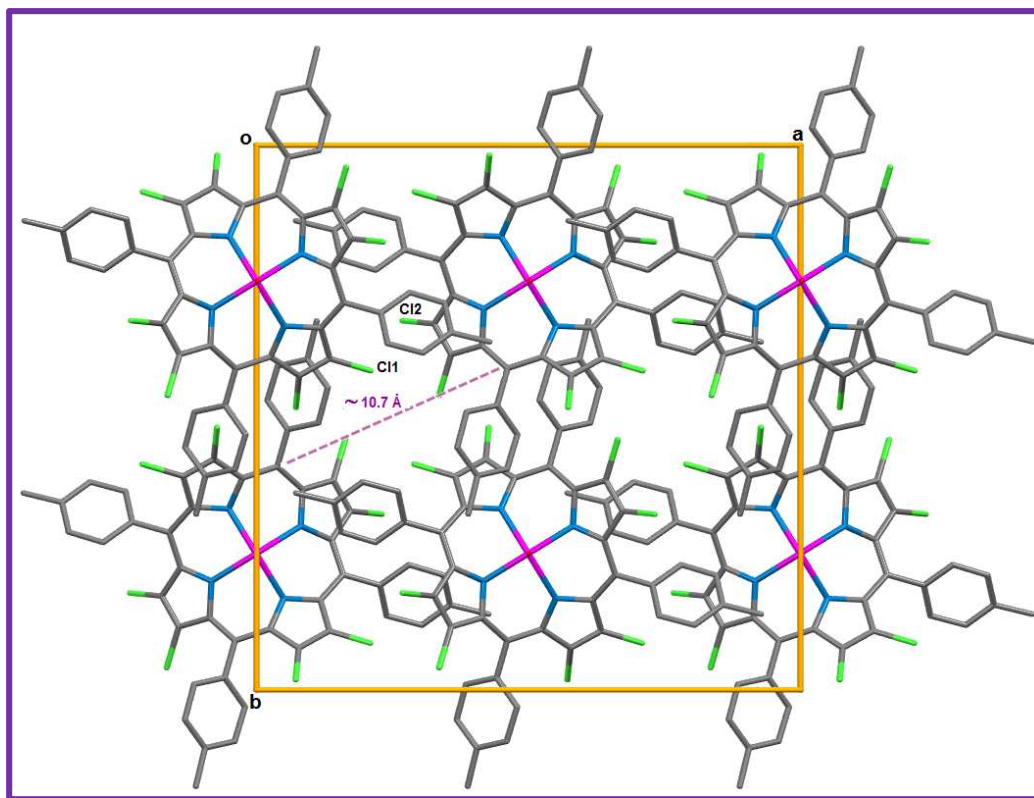[a]: D = donor atom, [b]: A = acceptor atom.

Figure 7. Partial packing of (**I**) showing channels parallel to the c axis.

4. Conclusion

The coordination compound vanadium(IV) oxo octachloro-*meso*-(4-tolylporphyrin) with the formula [V(Cl$_8$TTP)O] (**I**) was synthesized and its crystal structure was determined. We have shown that the β-pyrrole chloronation of the oxo[*meso*-(4-tolylporphyrinato)]vanadium(IV) complex [V(TTP)O] can be achieved quite easily by reacting, under ambient conditions, this species with an excess of thionyl chloride. The β-pyrrole chlorine substituents produce dramatic redshifts of the Soret and Q absorption bands of (**I**) and causes an anodic shift of the ring oxidation and reduction potentials of our vanadyl-Cl$_8$TTP derivative. This is explained by the electron-withdrawing property and the bulkiness of the chlorine atoms at the β-pyrrole positions of the porphyrin which causes an important deformation of the porphyrin core (especially the *saddle* distortion) of complex (**I**) in solution. Consequently, the HOMO orbital of the oxo metalloporphyrin is destabilized, while the LUMO orbital of the same species is practically unchanged, leading to a decrease of the HOMO-LUMO energy. The supramolecular structure of (**I**) is made by one-dimensional chains along the [001] made by [V(Cl$_8$TTP)O] molecules where are located channels parallel to this direction.

Acknowledgement

Supplementary Material

The crystallographic information file (abbreviated CIF) loading the data sets for (**I**) has been deposited with the Cambridge Structural Database(CSD), under deposit codes CCDC1532095(copies of these data may be obtained free of charge from The Director, CCDC, 12 Union Road, Cambridge CB2 1EZ, UK, Fax: ± 44 1223 336033; Email: deposit@ccdc.cam.ac.uk or http://www. ccdc.ac.uk)

References

[1] H.J. Callot, Bromuration de la *méso*-tétraphénylporphine structure et réactivité des produits, Tetrahedron Lett. 50 (1973) 4987-4990.

[2] J.P. Renoud, P. Battioni, J.F. Bartoli, D. Mansuy, A very efficient system for alkene epoxidation by hydrogen peroxide : Catalysis by manganese porphyrins in the presence of imidazole, J. Chem. Soc., Chem. Commun. (1985) 888-889.

[3] D. Mansuy, The Activation of dioxygen and homogeneous catalytic oxidation
eds. D.H.R. Barton, A.E. Martell and D.T. Sawyer, Plenum. New York, (1993) 347-358.

[4] T. Takeuchi, H.B. Gray, W.A. Goddard, Electronic Structures of halogenated porphyrins:
Spectroscopic Properties of ZnTFPPX8 (TFPPX8 = octa-β-halotetrakis(pentafluoropheny1)porphyrin; X = C1, Br), J. Am. Chem. Soc. 116 (1994) 9730-9732.

[5] Y. Fang, P. Bhyrappa, Z, Ou, K.M. Kadish, Planar and Nonplanar Free-Base Tetraarylporphyrins:
β-Pyrrole Substituents and Geometric Effects on Electrochemistry, Spectro electrochemistry, and Protonation/Deprotonation Reactions in Nonaqueous Media, Chem. Eur. J. 20 (2014) 524 – 532.

[6] S.A. Taghavi, M. Moghadam, I. Mohammadpoor-Baltork, S. Tangestaninejad, V. Mirkhani, A.R. Khosropour, Investigation of catalytic activity of high-valent vanadium(IV) tetraphenylporphyrin: A new, highly efficient and reusable catalyst for acetylation of alcohols and phenols with acetic anhydride, Inorg. Chemica Acta. 377 (2011) 159-164.

[7] S. Shigeta, S. Mori, E. Kodama ,J. Kodama, K. Takahashi,T. Yamase, Broad spectrum anti-RNA virus activities of titanium and vanadium substituted polyoxotungstates, Antiviral Res. 58 (2003) 265.

[8] D. Afzal, R. Baughman, A. James,M. Westmeyer,Synthesis and structural studies of early transition metalloporphyrin complexes. X-ray structures of *meso*-5,10,15,20-tetratolyl hafnium(IV) p-dioxo dimer complex and *meso*-5,10,15,20-tetratolylporphyrin vanadium(IV) oxo complex, Supramol. Chem. 6 (2006) 395-399.

[9] SADABS; Bruker (2015). APEX3, SAINT and SADABS. Bruker AXS Inc., Madison, Wisconsin, USA.

[10] M.C. Burla, R. Caliandro, M. Camalli, B. Carrozzini, G.L. Cascarano, L. De Caro, C. Giacovazzo, G. Polidori, R. Spagna, SIR2004: an improved tool for crystal structure determination and refinement ,J. Appl. Cryst. 38 (2005) 381-388.

[11] G.M.Sheldrick, Crystal structure refinement with SHELXL, Acta Cryst. A64 (2008) 112-122.

[12] P. Bhyrappa, V. Krishnan, Octabromotetraphenylporphyrin and its metal derivatives: Electronic structure andelectrochemical properties, Inorg. Chem. 30(1991)239-245.

[13] P. Hoffmann, G. Labat, A. Robert, B. Meunier, Spagna, highly selective bromination of tetramesitylporphyrin: an easy access to robust metalloporphyrins, M-Br$_8$TMP M-Br$_8$STMPS. examples of application in catalytic oxygenation and oxidation reactions, Tetrahedron Lett. 31 (1990) 1991-1994.

[14] V.D. Rumyantseva, E.A. Aksenova, O.N. Ponamoreva, A.F. Mironov,Halogenation of metalloporphyrins, Russ. J. Bioorg. Chem. 26 (2000) 471-477.

[15] R Kumar, N. Chaudhary, M.R. Maurya, M. Sankar, CSD Communication (Private Communication) (2015), CCDC 1420177, refcode PUNMIW.

[16] A. Ghosh , I. Halvorsen , H.J. Nilsen , E. Steene , T. Wondimagegn, R. Lie , E.V. Caemelbecke , N. Guo, Z. Ou, K.M. Kadish, Electrochemistry of nickel and copper β-octahalogeno-*meso*-tetraarylporphyrins. Evidence for important role played by saddling-induced metal (dx^2-y^2)-porphyrin ("a$_{2u}$") orbital interactions, J. Phys. Chem. B.105 (2001) 8120-8124.

[17] H.J. Callot, Bromination of m-tetraphenylporphine. Preparation of alkyl derivatives and polycyanoporphines. Bull. Soc. Chim. Fr. 69 (1974) 1492–1496.

[18] H.J. Callot, Nouvelles voies d'accès aux vinylporphyrines, Tetrahedron Lett. 29 (1973) 899-901.

[19] R. Weiss, J. Fischer, V. Bulach , V. Schunemann , M. Gerdan , A.X. Trautwein , J.A. Shelnutt , C.P. Gros , A. Tabard , R. Guilard , Structure and mixed spin state of the chloroiron(III) complex of 2,3,7,8,12,13,17,18-octaphenyl-5,10,15,20-tetraphenylporphyrin, Fe(DPP)Cl, Inorg. Chim. Acta 337 (2002) 223-232.

[20] G.A. Spyroulias, A.P. Despotopoulos, C.P. Raptopoulou, A. Terzis, D. de Montauzon, R. Poilblanc, A.G. Coutsolelos, Comparative study of structure properties relationship for Novel β-halogenated lanthanide porphyrins and their nickel and free bases precursors, as a function of number and nature of halogens atoms, Inorg. Chem. 41 (2002) 2648-2659.

[21] I.K. Thomassen, H. Vazquez-Lima, K.J. Gagnon, A. Ghosh,Octaiodoporphyrin, Inorg. Chem.54 (2015) 11493–11497.

[22] E.R. Birnbaum, J.A. Hodge, M.W. Grinstaff, W.P. Schaefer, L. Henling, J.A. Labinger, J.E. Bercaw, H.B. Gray, ^{19}F NMR spectra and structures of halogenated porphyrins, Inorg.Chem.34 (1995) 3625-3632.

[23] F. D'souza, A. Villard, E. Van Caemelbecke, M. Franzen, Boschi, P. Tagliatesta, K.M. Kadish, Electrochemical and Spectroelectrochemical Behavior of Cobalt(III), Cobalt(II), and Cobalt(I)

Complexes of *meso*-Tetraphenylporphyrinate Bearing Bromides on the β-Pyrrole Positions, Inorg. Chem. 32 (1993) 4042-4048.

[24] C.M. Che, J.L. Zhang, .Zhang, J.S. Huang, T.S. Lai, W.M. Tsui, X.G. Zhou, Z.Y. Zhou, N. Zhu, C.K. Chang, Hydrocarbon oxidation by β-halogenated dioxoruthenium(VI) porphyrin complexes: effect of reduction potential (RuVI/V) and C−H bonddissociation energy on rate Constants, J .Chem. Eur. 11 (2005) 7050-7053.

[25] T. Wijesekera, A. Matsumoto, D. Dolphin, D.L. Angen, Perchlorinated and highly chlorinated *meso*-tetraphenylporphyrin, Chem Int. Ed. Engl. 29 (1990) 1028-1030.

[26] A. Giraudeau, H.J. Callot, M. Gross, Effects of electron-withdrawing substituents on the electrochemical oxidation of porphyrins, Inorg. Chem. 18 (1979) 201-206.

[27] D. Mandon, P. Ochsenbein, J. Fischer, R. Weiss, K. Jayaraj, R.N. Austin, A. Gold, P.S. White, O. Brigaud,P Battioni,D. Mansuy,β-Halogenated-pyrrole porphyrins. Molecular structures of 2,3,7,8,12,13,17,18-octabromo-5,10,15,20-tetramesitylporphyrin,nickel(II)2,3,7,8,12,13,17,18-octabromo-5,10,15,20-tetramesitylporphyrin, and nickel(II) 2,3,7,8,12,13,17,18-octabromo-5,10,15,20-tetrakis(pentafluorophenyl)porphyrin, Inorg. Chem. 3 (1992) 2044-2049.

[28] O. Brigaud, P. Battioni, D. Mansuy, C. Giessner-Prette, Structure of *meso*-tetraaryl-β-octahalogeno-porphyrins : a semi-empirical quantum mechanical investigation, New Journal Chem. 16 (1992) 1031-1038.

[29] K.M. Kadish, M.M. Morrison, Solvent and substituent effects on the redox reactions of *para*-substituted tetraphenylporphyrin, J. Am. Chem. Soc. 98 (1976) 3326-3328.

[30] K.M. Kadish, M.M. Morrison, Substituent effects on the redox reactions of tetraphenylporphyrins, Bioinorg. Chem. 7 (1977) 107-115.

[31] W.R. Scheidt, Y. Lee, Recent Advances in the Stereochemistry of Metallotetrapyrroles, Struct. Bonding (Berlin), 64 (1987) 1-7.

[32] M.P. Byrn, C.J Curtis, Y. Hsiou, S.I. Khan, P.A Sawin, S.K. Tendick, A. Terzis, C.E. Strouse, Porphyrin sponges: conservation of host structure in over 200 porphyrin-based lattice Clathrates, J. Am. Chem. Soc. 115 (1993) 9480-9491.

[33] P. Bhyrappa, V. Krishnan, M. Nethaji, Solvation and Axial ligation properties of (2,3,7,8,12,13,17,18-octabromo-5,10,15,20-tetraphenylporphyrinato)zinc(II), J. Chem. Soc. Dalton Trans.(1993) 1901-1906.

[34] E.R. Birnbaum, J.A Hodge, M.W. Grinstaff, W.P. Schaefer, L. Henling, J.A. Labinger, J.E. Bercaw, H.B. Gray, ^{19}F NMR spectra and structures of halogenated porphyrins, Inorg. Chem. 34 (1995) 3625-3632.

[35] R.E. Marsh, W.P. Schaefer, J.A. Hodge, M.E. Hughes, H.B. Gray, J.E. Lyons, A. Highly solvated zinc(II) tetrakis-(pentafluorophenyl)-β-octabromoporphyrin, Acta Cryst. C49 (1993) 1339-1342.

[36] Z. Li, Y. Hu, T. Li Crystal structure and third-order nonlinear optical properties study of tetraphenylporphyrinand its nickle complex at wavelength 532 nm and 1064 nm Mol Cryst. Liq. Cryst. 605 (2014) 135–145.

[37] R. Patra, D. Sahoo, S. Dey, D. Sil, S.P. Rath, switching orientation of two axial imidazole ligands between parallel and perpendicular in low-spin Fe(III) and Fe(II) nonplanar porphyrinates, Inor. Chem 51 (2012) 11294-11305.

[38] M.W. Grinstaff, M.G. Hill, E.R. Birnbaum, W.P. Schaefer, J.A. Labinger, H.B. Gray, Structures, Electronic Properties, and Oxidation-Reduction Reactivity of Halogenated Iron Porphyrins, Inorg. Chem. 34 (1995) 4896-4902.

[39] M.G.B Drew, P.C.H Mitchell, C.E. Scott, Crystal and molecular structure of three oxovanadium(IV)porphyrins:oxovanadiumtetraphenylporphyri (I) oxovanadium(IV) etioporphyrin (II) and the 1: 2 adduct of (II) with 1,4-dihydroxybenzene(III). Hydrogen bonding involving the VO group. Relevance to catalytic demetallisation, Inorg. Chim. Acta. 82 (1984) 63-68.

[40] L.M. Berreau, J.A Hays, V.G Young, Junior, L.K. Woo, Synthesis of early transition metal porphyrin halide complexes: first structural characterization of a vanadium(III) porphyrin complex, Inorg. Chem.33 (1994) 105-108.

[41] R. Harada, H. Okawa, T. Kojima, Synthesis, characterization, and distortion properties of vanadyl complexes of octaphenylporphyrinand dodecaphenylporphyrin, Inorg.Chim.Acta. 358 (2005) 489-496.

[42] G. Nandi, H.M. Titi, I. Goldberg, Exploring supramolecular self-assembly of metalloporphyrin tectons by halogen bonding, Cryst.Growth Des. 14 (2014) 3557–3566.

[43] Y.P. Peia, J.G Huanga, R.H. Hua, Y.X. Yanga, J. Zhoua, W.T. Chen, Metal-induced property variation for a series of lanthanide vanadium porphyrins, J. Porphyrins Phthalocyanines, 19 (2015) 1-8.

- Preparation of the β-pyrrole oxo octachloro-*meso*-tetratoloylporphyrinato vanadium(IV) complex (**I**) using an easy method by reaction the oxo *meso*-tetratoloylporphyrinato vanadium(IV) starting material with an excess of $SOCl_2$.

- UV-visible spectrum shows important redshifted Soret band of (**I**).

- Voltammogram of (**I**) exhibits important anodic shift of the porphyrin ring oxidation and reduction potentials.

- The molecular structure of (**I**) shows a very high saddle distortion and an important ruffled deformation of the porphyrin macrocycle.